A New Enzyme Model For Enantioselective Esterases Based On Molecularly Imprinted Polymers

Marco Emgenbroich and Günter Wulff*[a]

Dedicated to Professor Kurt Mislow on the occasion of his 80th birthday.

Abstract: An efficient enzyme model exhibiting enantioselective esterase activity was prepared by using molecular imprinting techniques. The enantiomerically pure phosphonic monoesters **4L** and **5L** were synthesized as stable transition-state analogues. They were used as templates connected by stoichiometric noncovalent interactions to two equivalents of the amidinium binding site monomer **1**. After polymerization and removal of the template, the polymers were efficient catalysts for the hydrolysis of certain nonactivated amino acid phenylesters (**2L**, **2D**, **3L**, **3D**) depending on the template used. Imprinted catalyst **IP4** (imprinted with **4L**) enhanced the hydrolysis of the corresponding substrate **2L** by a factor of 325 relative to that of a buffered solution. Relative to a control polymer containing the same functionalities, prepared without template **4L**, the enhancement was still about 80-fold, showing the highest imprinting effect up to now. In cross-selectivity experiments a strong substrate selectivity of higher than three was found despite small differences in the structure of the substrate and template. Plots of initial velocities of the hydrolysis versus substrate concentration showed typical Michaelis–Menten kinetics with saturation behavior. From these curves, the Michaelis constant K_M and the catalytic constant k_{cat} can be calculated. The enantioselectivity shown in these values is most interesting. The ratio of the catalytic efficiency k_{cat}/K_M, between the hydrolysis of **2L**- and **2D**-substrate with **IP4**, is 1.65. This enantioselectivity derives from both selective binding of the substrate ($K_ML/K_MD = 0.82$), and from selective formation of the transition state ($k_{cat}L/k_{cat}D = 1.36$). Thus, these catalysts give good catalysis as well as high imprinting and substrate selectivity. Strong competitive inhibition is caused by the template used in imprinting. This behavior is also quite similar to the behavior of natural enzymes, for which these catalysts are good models.

Keywords: enzyme catalysis · enantioselectivity · enzyme models · molecular imprinting · transition-state analogue

Introduction

In order to prepare a catalyst that works similarly to an enzyme, a cavity that functions as an active site has to be generated with a shape corresponding to the shape of the substrate or, even better, to the shape of the transition state of the reaction. Furthermore, functional groups have to be introduced into this cavity in an accurate three-dimensional orientation in order to be effective as binding sites, coenzyme analogues, or catalytic sites.

Previously, we have introduced a novel method for obtaining such structures in synthetic polymers ("enzyme-analogue built polymers").[1, 2] For this, a highly cross-linked copolymer is formed around a template molecule. The monomer mixture contains functional monomers that can interact with the template through covalent or non covalent interactions. After removal of the template, an imprint containing functional groups in a certain orientation remains in the polymer. The shape of the formed imprint, and the arrangement of the functional groups are complementary to the structure of the template (for reviews see ref. [3–5]).

For the preparation of imprinted polymeric catalysts, the functional groups to be introduced should act as binding and catalytically active sites. Furthermore, it is necessary to create a shape of the cavity that will support the catalysis, for example, by stabilizing the transition state of the reaction. This approach was inspired by the results of Schulz, Lerner, and others, by generating antibodies against stable transition-state analogues of a reaction, and obtaining catalytically active antibodies.[6, 7] In addition to the special shape of the active site in the antibodies, catalytic antibodies possess, similar to that in enzymes, special catalytically-active functional groups like guanidine groups, that considerably enhance the catalytic reaction. Since most of the research in antibody chemistry is concerned with ester hydrolysis, these reactions were the first to be investigated in molecular

[a] Prof. Dr G. Wulff, Dr. M. Emgenbroich
Institute of Organic Chemistry
and Macromolecular Chemistry
Heinrich-Heine-University
Düsseldorf, Universitätsstrasse 1
40225 Düsseldorf (Germany)
Fax: (+49) 211-811-5840
E-mail: wulffg@uni-duesseldorf.de

DOI: 10.1002/chem.200304783

imprinting.[8–12] (for a recent review see ref [13]). The main problem to generate an efficient enzyme model by molecular imprinting is to find a suitable template array that contains the stable transition-state analogues, the binding sites, and catalytically-active groups in the desired position.

One possible way to solve this problem is to use noncovalent interactions between templates and binding-site monomers with high association constants (so-called stoichiometric noncovalent interactions), like the binding of amidine groups with carboxylic acid, phosphonic acid, or phosphoric acid groups.[14, 15] In this respect, it is interesting to note that the most active esterase species among catalytic antibodies contain a guanidinium group (of the amino acid L-arginine), which plays an important role in catalyzing the basic hydrolysis of esters.[16] Similarly, in the investigation of alkaline hydrolysis of esters, carbonates, and carbamates, we used amidine groups in polymeric catalysts for binding and catalysis.[9, 13, 17] We were able to obtain catalysts by molecular imprinting that showed enhancements in ester hydrolysis, 102–235 times faster relative to the solution reactions. In the case of carbonates and carbamates, the hydrolysis catalyzed by an imprinted polymer was 588 and 1400–3860 times faster, respectively. It could be shown that these catalysts exhibit Michaelis–Menten kinetics similar to enzymes. Further examples by using amidines in a similar way have recently been published.[18]

In the next step we now want to form a model for an enantioselective esterase, and consequently combine the well-known enantioselectivity in separation with the catalytic properties of the imprinted polymers.

Previously, Sellergren and Shea presented catalytically-active imprinted polymers for the hydrolysis of a chiral amino acid ester.[10, 11] The imprint was obtained by a combination of covalent and noncovalent interactions. A chiral α-amino phosphonate was used as the template. In order to mimic the catalytic triad of the active site in chymotrypsin, imidazole, phenolic hydroxy, and carboxyl groups were used as catalytically-active groups. Although the rate enhancements were not very high (2.5-fold vs control polymer, and 10-fold vs solution), the enantioselectivity for the hydrolysis was quite high at $k_D/k_L = 1.85$.

This paper describes the synthesis of enantiomerically pure template molecules, their corresponding substrates, and the preparation and catalytic properties of the molecularly-imprinted polymers.

Results and Discussion

Synthesis of the substrates and templates: Firstly we investigated the hydrolysis of an aromatic dicarboxylic monoester (4-carboxyphenylacetic(3,5-dimethylphenyl) ester), and used the corresponding phosphonic ester (4-carboxylbenzylphosphonic-mono-(3,5-dimethylphenyl) ester) as the stable transition-state analogue acting as the template. This template was converted into a bisamidinium salt with *N*,*N*′-diethyl(4-vinylphenyl)amidine (**1**) acting as the binding site monomer.[9] The amidinium groups are attached to the carboxyl group, as well as to the phosphonic monoester group of the template, by two chelated hydrogen bonds combined with electrostatic interaction. It was therefore possible to fix a transition-state analogue template during imprinting and, at the same time, position the amidine groups in the correct orientation for catalysis. To investigate a similar but non-racemic chiral system, the substrate should be based on α-amino acid derivatives that are easily available as both enantiomers. The ester residue should also contain a nonactivated 3,5-dimethylphenylester to create a significant imprint, and a 4-carboxybenzoyl group at the N-terminal part should be introduced.

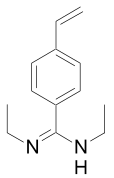

1

As a result, the free carboxylic acid can act as a binding motif during catalysis, and the hydrolysis products, phenol and dicarboxylic acid, can easily be detected by UV absorption during HPLC separations. Therefore, the *N*-(4-carboxybenzoyl)-α-amino acid (3,5-dimethylphenyl) esters **2** and **3**, derived from L- and D-leucine and L- and D-valine were prepared as substrates.

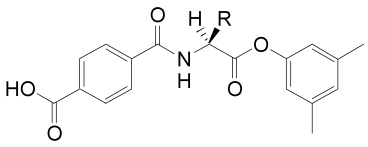

2L R= isobutyl
3L R= isopropyl

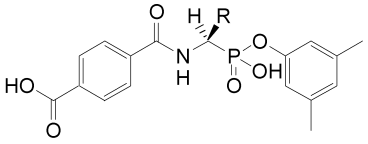

4L R= isobutyl
5L R= isopropyl

The synthesis started from commercially available carbobenzoxy protected α-amino acids, which were transformed into 3,5-dimethylphenyl esters **6** and **7** by coupling in the presence of (benzotriazol-1-yloxy)tris(dimethylamino)phosphonium hexafluorophosphate (BOP)[19] and *N*-methyl morpholine (see Scheme 1). After deprotection of the N-terminal group with 33% HBr in acetic acid, the hydrobromides **8** and **9** (as L and D forms) were obtained. Hydrobromides **8** and **9** were coupled in the presence of chlorotripyrrolidinophosphonium hexafluorophosphate (PyCloP)[20] with monobenzyl terephthalic acid (**10**) to obtain the amides **11** and **12**. The substrates **2** and **3** (in both enantiomeric forms) were obtained by hydrogenolytic fission of the benzyl esters.

The synthesis of the optically active templates **4** and **5** (see Scheme 2) was somewhat more laborious. The two most common ways to build up a chiral α-amino phosphonic acid are either by fractionated crystallization of diastereomeric salts,[21] or synthesis by a diastereoselective reaction.[22] Both were tested successfully in our laboratory. We chose the synthesis of chiral α-L-amino phosphonic acid diethyl esters starting from *O*-methyl-D-phenylglycinol, as described by Smith et al.[22] By varying the reaction conditions, we were able to improve the yield and diastereomeric excess of the reaction, after column chromatography, for **13** and **14**. To build up our molecules, the N-terminal in **13** and **14** was

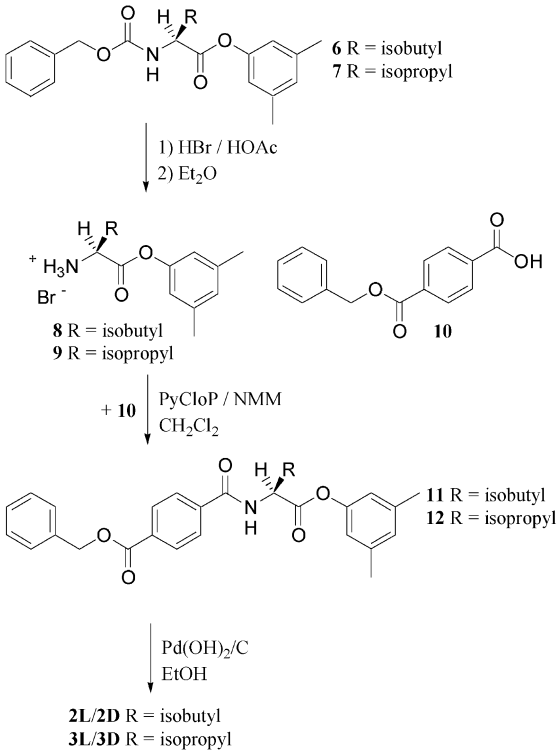

Scheme 1. Synthesis of the substrate molecules based on valine and leucine. All molecules were prepared in both enantiomeric forms, inscribed with D and L for the corresponding forms.

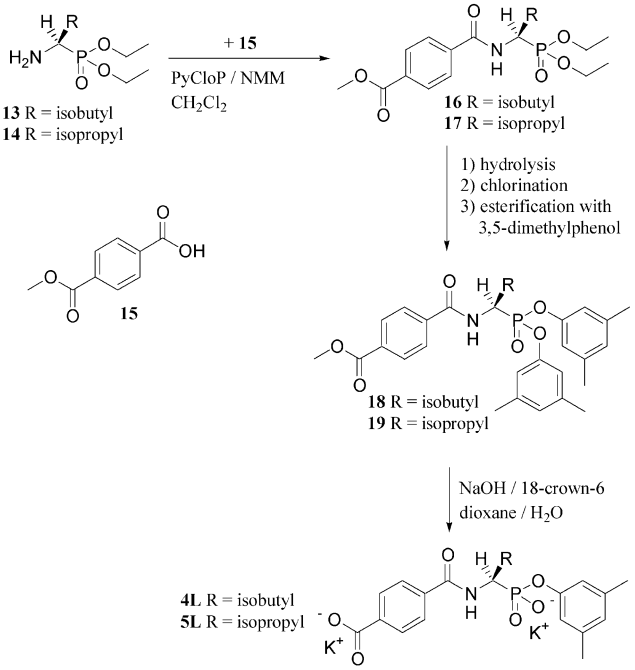

Scheme 2. Synthesis of the transition-state analogues (template molecules) for valine- and leucine-based substrates (only L forms).

coupled with monomethyl terephthalic acid (**15**) to prepare **16** and **17**. To modify the P-terminal part of the phosphonic acid diethyl esters, they were hydrolyzed by bromotrimethylsilane[23] in order to yield the free phosphonic acid, which was dried, directly chlorinated with oxalylchloride, and esterified with two equivalents of 3,5-dimethylphenol to obtain the diesters **18** and **19**. The last step was a combined hydrolysis of the carboxylic methyl ester and diphenyl ester to yield the corresponding monophenyl ester; this was performed analogously according to reference [24] with sodium hydroxide activated by [18]crown-6 in dioxane/water 1:1 (v/v). The products **4** and **5** were purified by column chromatography under basic conditions, and transformed into the dipotassium salts by an ion exchange column procedure. This workup procedure was necessary, since the monoesters were not stable under acidic conditions.

Synthesis and catalytic properties of imprinted and control polymers: Earlier investigations showed that the amidinium monomer **1** forms complexes with carboxylic acids and phosphonic monoesters in acetonitrile with high association constants. In less polar solvents, like toluene, the association constant is even higher.[14, 15] From this data it can be calculated that in toluene/acetonitrile (1:1), under polymerizing conditions to form imprinted polymers, more than 97% of the acidic groups in **4L** and **5L** are complexed if a 1:2 molar mixture of template and **1** is present. This stoichiometric noncovalent interaction further assures that nearly no unbound amidines are present in the polymerizing mixture. Thus, imprinted polymers are prepared from **4L** and **5L** as templates with the addition of two equivalents of **1** (see Scheme 3). The copolymerization with ethylenedimethacrylate (EDMA) and methylmethacrylate (MMA) is performed in the usual way by radical initiation (see Table 1).

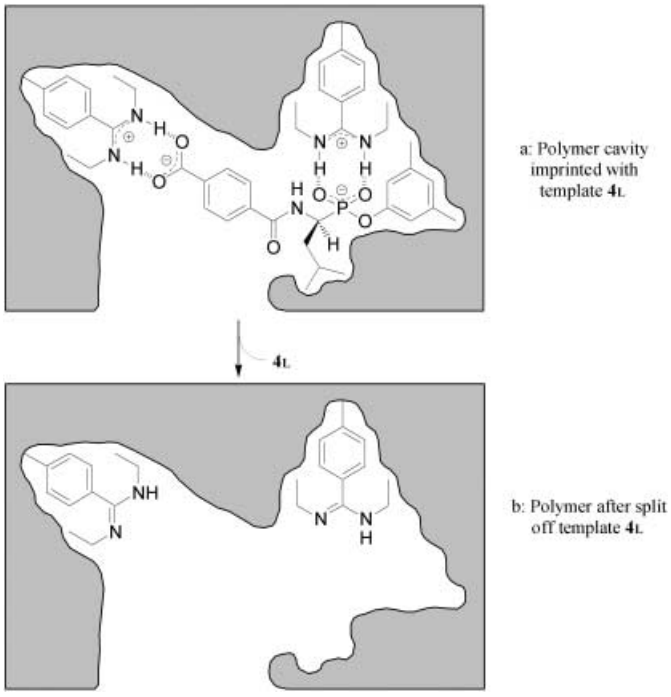

Scheme 3. Model of an imprinted cavity with template **4L**, and two equivalents of the binding site monomer **1**.

Control polymers are prepared under identical conditions with the same amount of the amidine monomer **1**, but without templates **4L** and **5L**. The polarity and the polymerization behavior of **1** is different from the complexed monomers, to

Table 1. Polymer composition and properties[a]

Polymer	Amount [g]		Splitting off the template [%]		Inner surface area [m^2/g]
	complex	template	by HPLC	by titration	
IP4	0.300	**4L** 0.155	76	75	217
IP5	0.300	**5L** 0.155	92	82	196
CPB	0.160	benzoic acid 0.037	95	92	287
CPF	0.137	formic acid 0.014	–	82	276

[a] The composition of the monomer mixture for the preparation of the imprinted polymers, consisted in all examples of EDMA (8.20 g, 7.81 mL), MMA (1.50 g, 1.59 mL), **1** (0.123 g) or **1**-HCl (0.144 g) (**IP4** and **IP5**), AIBN (0.10 g), and as porogene a mixture of toluene (5 mL) and acetonitrile (5 mL). The type and amount of template varied as shown in the Table. The complex is formed from the template and **1;** here the amount is calculated. For the determination of the percentage of splitting off see the Experimental Section. Inner surface area was measured by BET (N_2) one point measurement (particle size 45–125 μm).

overcome this difficulty we used simple carboxylic acids for complexing, such as formic acid and benzoic acid. To some extent these acids also behave as templates, especially benzoic acid; however, they only possess one carboxylic group per molecule and do not have the required transition-state shape. Thus, the differences in their performance give good indications of the imprinting effects.

The polymers are prepared by radical initiation in an ampoule, and are produced as solid macroporous blocks, which are then crushed, ground, and sieved to obtain a particle size of 45–125 μm. The polymers are all macroporous with high inner-surface areas (196–287 $m^2 g^{-1}$), as is typical for these type of polymers (see Table 1). The template is then split off by repeated washing with a 1:1 mixture of 0.1M sodium hydroxide and methanol. From HPLC, it was determined that 75–95% of the templates could be released from the polymer. Alternatively, the amount of accessible amidine groups was determined by titration after splitting off the templates (see Table 1). Both methods gave comparable results, in the case of **IP5** there was some deviation.

The conditions for the application of imprinted polymer catalysts with amidine-based binding site monomers have previously been optimized.[17] The hydrolysis of the esters was carried out under these optimal conditions in a 1:1 mixture of a 2-[4-(2-hydroxyethyl)-1-piperazino]ethanesulfonic acid (HEPES) buffer, at pH 7.3, with acetonitrile (20 °C). For this purpose, a freshly prepared substrate solution of 1×10^{-3} M in acetonitrile was added to a suspension of catalyst containing 2×10^{-3} M active sites (containing 4×10^{-3} M accessible amidine groups). The hydrolysis of both enantiomers was always determined separately to check for enantioselectivity.

In the case of the control experiments, an amount of dry control polymer with the same amount of accessible amidine groups was used. The hydrolysis in solution, without any polymer catalyst, was carried out in the same buffer solution mixture, and at the same substrate concentrations. Control experiments with monomeric binding sites *N,N′*-diethyl-4-vinylbenzamidine (**1**) in buffered solutions were not performed, since earlier experiments showed that the amidine groups hardly exert any catalytic effect in buffered solution, because most of these groups are protonated at this pH value.[9]

To follow the reaction kinetics, aliquots were taken at regular intervals and checked by HPLC. The reaction rate constants for the hydrolysis were measured during conversion of the first 5 to 10% of substrate conversion, while the reaction rate was in the linear range. The catalytic activity of **IP4** was checked at two different buffer concentrations of 0.1M and 0.15 M. The kinetics can be treated as a pseudo-first-order reaction, since the concentration of hydroxide ions during the reaction is constant. To follow the reaction, the phenol product was chosen for detection monitoring, because it shows no product inhibition and should be released from the catalyst.

The reaction is described by Equation (1).

$$RCOOR' + OH^- \longrightarrow RCOO^- + R'OH \quad (1)$$

For pseudo-first-order kinetics, Equation (2)[25] can be used.

$$\ln\left[\frac{[RCOOR']_{t=0} - [R'OH]_t}{[RCOOR']_{t=0}}\right] = -kt \quad (2)$$

The reactions were repeated 2–3 times, and the given data consists of average values shown with the standard deviation. The data for k was obtained by linear regression of at least 6–9 data points at different time intervals with correlation coefficients from 0.980–0.999.

Figure 1a and b show the observed calculated pseudo-first-order kinetics for the hydrolysis of **2L** and **2D** under catalysis of the imprinted polymer **IP4**, relative to the control experiments. A strong catalytic activity of **IP4** for the hydrolysis of the substrate **2L** is observed. The catalysis with the control polymer **CPF** and the reaction in solution are much slower. Similar results are obtained for the second polymer **IP5** imprinted with the valine analogue template **5** (see Figure 2a and b). The values calculated from the slopes in Figures 1 and 2 are given in the Experimental Section. The ratios of these reaction constants result in relative enhancements in reaction rate constants, as shown in Tables 2 and 3. Based on these results, one can point out that the polymer **IP4**, imprinted with the L-leucine-analogue amino phosphonic acid **4**, accelerated the hydrolysis of the L-substrate **2L** in relation to the solution by factors from 200 to 325 times depending on the buffer concentration. It was observed that the buffer concentration had a strong influence on the reaction rate constants. At a lower buffer concentration, the relative reaction rate constants increase by a factor of around 1.5 relative to a buffer solution without a catalyst. This results in higher selectivity.

The enhancements show a strong catalytic effect of the imprinted polymers relative to the solution. These enhancements might not be solely caused by an imprinting effect.

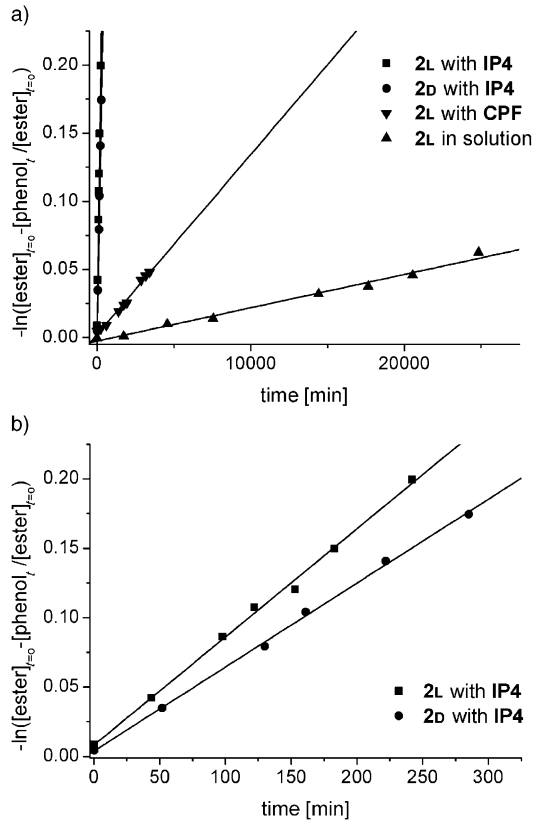

Figure 1. a) Comparison of the measured pseudo-first-order kinetics for the hydrolysis of leucine substrates **2L** and **2D**, in the presence of **IP4**, **CPF**, and just in solution. (In all cases: actetonitrile/0.1N HEPES buffer pH 7.3, 1:1) b) Pseudo-first-order kinetics for hydrolysis of leucine substrates **2L** and **2D** in the presence of **IP4**.

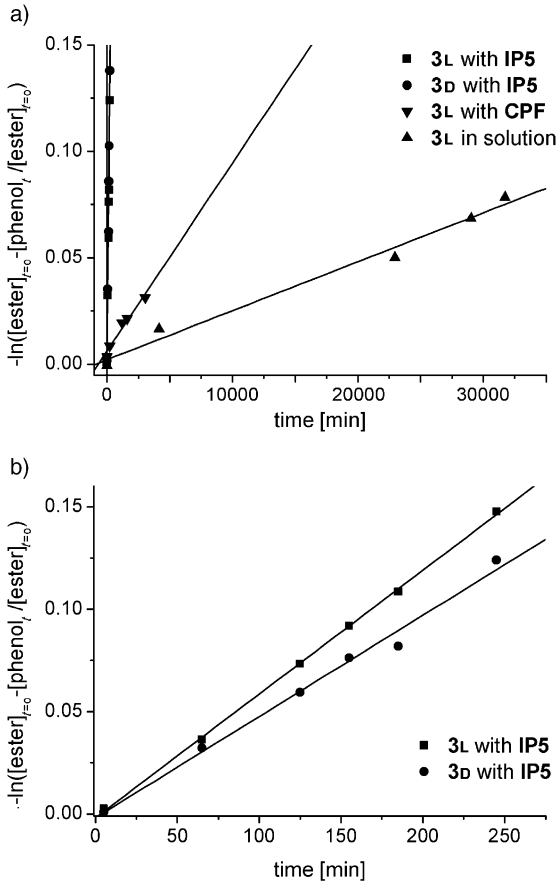

Figure 2. a) Comparison of the measured pseudo-first-order kinetics for the hydrolysis of valine substrate **3L** and **3D**, in the presence of **IP5**, **CPF**, and just in solution. (Solvent same as in Figure 1a). b) Pseudo-first-order kinetics for the hydrolysis of leucine substrates **3L** and **3D**, in the presence of **IP5** (Solvent same as in Figure 1a).

Possible effects of the polymer backbone and binding sites, without a specific imprinting effect, can be elucidated by investigation of the control polymers. The differences between the catalytic activity of imprinted and control polymers correspond to the imprinting effect.[13] Polymer **IP4** showed a high enhancement, 67 to 79 times, relative to the control polymer **CPF**; this was dependant on the buffer concentration during the experiment. The acceleration relative to the second control polymer **CPB** was about 14. Thus, the activity of the control polymers was dependent on the size of the complexing acid. By enlarging the template in the control polymer (from formic acid to benzoic acid), a small imprinting effect was observed.[9]

Table 3. Relative enhancements and enantioselectivities for the hydrolysis of substrates **3L** and **3D** in acetonitrile/0.1M HEPES buffer pH 7.3 (1:1) at 20°C, by using **IP5** and the controls **CPF** and solution.

	Substrate	Relative enhancements[a]	Enantioselectivity L versus D
IP5 vs solution	**3L**	249	1.21
IP5 vs solution	**3D**	206	
IP5 vs **CPF**	**3L**	59	
CPF vs solution	**3L/3D**	4.2	

[a] Relative reaction rate constants = relative enhancements between **IP5**, **CPF** and solution.

Table 2. Relative enhancements and enantioselectivities for the hydrolysis of substrates **2L** and **2D** in acetonitrile/HEPES buffer pH 7.3 (1:1) at 20°C, by using **IP4** and the controls **CPF**, **CPB**, and solution in two different buffer concentrations (0.15 and 0.10M).

		HEPES buffer 0.15M		M HEPES buffer 0.10	
	Substrate	Relative enhancements[a]	Enantioselectivity L versus D	Relative enhancements	Enantioselectivity L versus D
IP4 vs solution	**2L**	325	1.39	200	1.20
IP4 vs solution	**2D**	234		166	
IP4 vs **CPF**	**2L**	79		67	
IP4 vs **CPB**	**2L**	14		–	
CPB vs solution	**2L/2D**	24		–	
CPF vs solution	**2L/2D**	4.1		3.0	

[a] Relative reaction rate constants = relative enhancements between **IP4**, **CBF**, **CPB** and solution.

While the hydrolysis reaction is enhanced 325-fold with an imprinting effect of 79 in a 0.1 M HEPES buffer by **IP4**, the enantioselectivity between the L- and D-substrates (defined as the ratio from the reaction rate constants of the hydrolysis of the L- versus the D-enantiomer), catalysed by polymer **IP4** is 1.39. Thus a significant enantioselectivity is observed. This clearly shows that there is substrate selectivity in these imprinted polymers. Table 3 shows that similar, though somewhat lower values are obtained for the imprinted catalyst **IP5**. In this case, the smaller substituent in the template seemed to cause a somewhat diminished imprinting accuracy.

Another way to examine the substrate selectivity is to measure the cross-selectivity. We checked the cross-selectivity of both L-imprinted polymers **IP4** and **IP5** with both corresponding L-substrates **2L** and **3L**. For this purpose, the catalytic effect for the hydrolysis of the L-valine-substrate **3L** by **IP4** (imprinted with the L-leucine analogue template **4**) and **2L** with **IP5** were investigated. As shown in Table 4, the

Table 4. Cross-selectivities of valine substrate **3L** in polymer **IP4** (leucine-analogue polymer), and leucine substrate **2L** in **IP5** (valine-analogue polymer) in acetonitrile/0.1M HEPES buffer pH 7.3 (1:1) at 20°C.

Catalyst	Substrate	k_{IP}/k_{sol}[a]	Cross-selectivity
IP4	**2L**[b]	325	3.2
IP4	**3L**[b]	103	
IP5	**3L**	249	3.2
IP5	**2L**	79	
IP4 vs. **IP5**	**2L**		4.2
IP5 vs. **IP4**	**3L**		2.5

[a] Relative enhancement of the imprinted catalyst *versus* solution [b] **2L** = L-leucine substrate; **3L** = L-valine substrate.

"wrong" substrate was clearly hydrolyzed slower in both cases. The cross-selectivity can be calculated in two different ways. If the cross-selectivity is defined as the quotient of the reaction rate constant for the hydrolysis of different substrates, with the same polymer used, this value was about 3 for both polymers. An alternative way to describe the cross-selectivity, which can be defined as the ratio of the reaction rate constant for the hydrolysis of one substrate by different polymers, gave values of 4.2 (leucine substrate **3L**) and 2.5 (valine substrate **4L**) (see Table 4). The enantioselectivity and the cross-selectivity show that the templates formed a specific catalytically active cavity that is able to distinguish between very similar substrates. It is surprising to realize that the difference of an isopropyl group and an isobutyl group results in 3 times more catalytic activity. In each case, the polymer imprinted with a leucine template analogue hydrolyzes the leucine ester considerably faster, and the polymer imprinted with a valine analogue hydrolyzes the valine ester considerably faster.

Mechanism of the catalytic action: In order to elucidate the mechanism of catalysis for the hydrolysis, a detailed kinetic investigation was performed. A plot of initial velocities of the reaction versus the substrate concentration was carried out for the hydrolysis of **2L** and **2D** in the presence of the imprinted catalysts **IP4**, as well as in the presence of control polymer **CPF** (see Figure 3). It was expected that it should also be

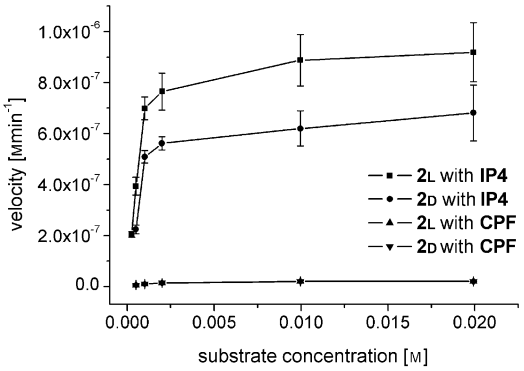

Figure 3. Michaelis–Menten kinetics illustrating the rate of hydrolysis for **2L** and **2D** in acetonitrile/0.1N HEPES buffer pH 7.3 (1:1), in the presence of **IP4** and **CPF**.

possible to get information on the extent of the influence of selective binding and selective catalysis on the enantioselectivity of the catalysis in this way.

Catalysis by **IP4** is shown in Figure 3, the curves in the graph resemble typical Michaelis–Menten curves (especially in the hydrolysis of **2L**). Therefore one can conclude, that, similar to enzyme catalysis, the substrate (ester) is bound to the catalyst in a pre-equilibrium step (see Scheme 4a). The bound ester is then converted by activation of the carbonyl group of the ester by one of the amidine groups, and the attacking water molecule; this occurs via a transition state

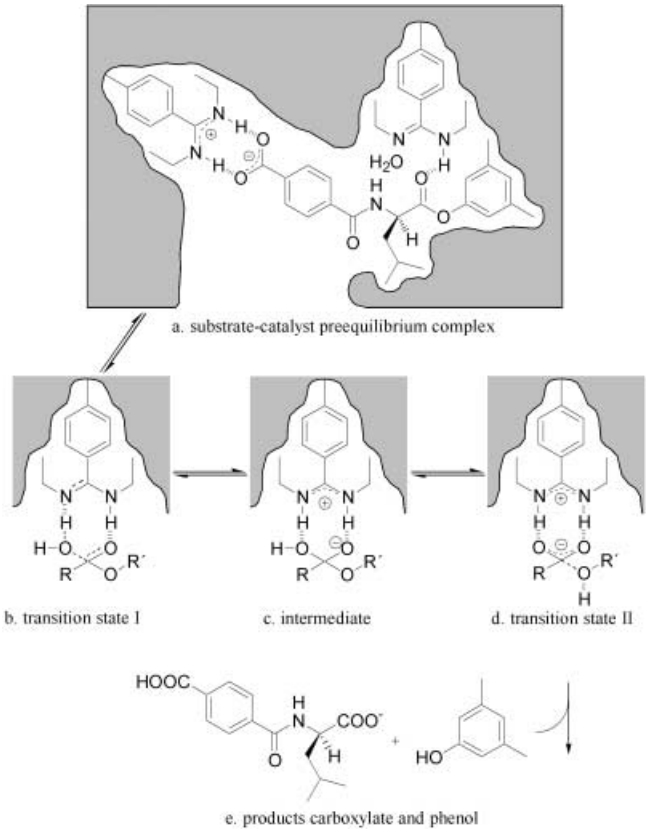

Scheme 4. Schematic picture of the different steps in the reaction pathway during the catalyzed hydrolysis of substrate **2L**, beginning with the substrate-catalyst complex a and the detailed view of the following steps b–e.

(Scheme 4b) to an intermediate similar to that in Scheme 4c. The energy difference between the transition state and the intermediate is small therefore, according to the Hammond rule, both structures are similar. This justifies why instead of a transition-state analogue, an intermediate analogue could be used as a template for the imprinting (compare Scheme 3a and Scheme 4b and c). The last step involves the breaking down of the tetrahedral intermediate via transition state II, to release the carboxylate and the alcohol according to Equation (1) (see Scheme 4c and d).

If the reaction is performed with increasing amounts of substrate (Figure 3), the rate of the reaction first increases with increasing substrate concentration, but then levels off. At higher substrate concentration, when all active sites are occupied, it remains constant, that is, it is zero-order with respect to the ester concentration (saturation kinetics). In contrast, the nonimprinted control polymer **CPF** exhibits a curve of low catalytic activity. From the curves shown in Figure 3, similarly as with enzymes, the influence of binding and catalysis can be elucidated by using the well-known Michaelis–Menten Equation (3):[25]

$$v_0 = \frac{k_{cat}[C][S]}{K_m + [S]} \quad (3)$$

in which, v_0 = initial rate; k_{cat} = rate constant of the catalyzed reaction, K_M = Michaelis constant, [S] = molar concentration of substrate, and [C] = total molar concentration of active sites in the catalyst.

To calculate meaningful values for K_M and k_{cat} poses some problems. Primarily, the kinetic measurements are carried out in a heterogeneous phase, which limits the accuracy of the values; this is especially true for kinetics at low substrate concentration. Therefore, we did not use linearization by a double reciprocal plot (Lineweaver–Burk plot), instead we used a computer program to fit the experimental values into Equation (3) representing a hyperbola. This usually gives values of higher accuracy.[26]

To solve Equation (3) the number of active sites in the imprinted polymers **IP4** and **IP5** should be determined. A first value is obtained by the determination of the amount, if template molecules were released from the imprinted polymer. Since the possibility of shrinking and nonaccessibility of cavities exists, this value has been further controlled by titration of the amidine groups with acid (see Table 1). Both methods gave similar values, indicating that with this stoichiometric noncovalent imprinting most of the cavities are available. Earlier work showed that in the case of bisamidinium bound templates, nearly the same amount of the template is taken up, as has been split off after imprinting.[14, 15]

A further problem in the calculation of data from Equation (3) exists. Unlike enzymes and monoclonal antibodies, imprinted catalysts have active sites with different binding ability, different selectivity in binding, as well as different catalytic activity. This inhomogeneity ("polyclonality") is especially effective if a strong excess of substrate is present, since all active sites are then occupied. For this reason mean values will be obtained; however, it is not exactly known how these averages are generated. From the appearance of the curve in Figure 3, a strong participation of the more active sites can be concluded. Values given for K_M and k_{cat} in the following paragraphs are therefore "apparent" values. Regardless of these difficulties, important conclusions can be drawn from the results obtained.

Table 5 shows the calculated data for k_{cat} and K_m. The Michaelis constant K_M, is a measure of the stability of the substrate–catalyst complex. Values for the template analogue substrate of 0.51 and 0.34 mM are found. This shows a relatively high stability of the substrate–catalyst complex, especially if it is taken into account that this noncovalent interaction occurs in a medium consisting of a mixture of aqueous buffer and acetonitrile in a 1:1 ratio. k_{cat} is the first-order rate constant, and is a measure of the catalytic activity of the catalyst. It corresponds to the number of reactions per minute an active site of the catalyst can catalyze (turnover number). With $k_{cat} = 4.74 \times 10^{-4}$ min^{-1} and 3.26×10^{-4} min^{-1}, these values are not very high. However, it should be taken into account that the hydrolysis of a relatively stable phenylester was investigated, unlike in many other investigations, in which the kinetics of the hydrolysis for 4-nitrophenylester was measured. For both polymers **IP4** and **IP5**, the substrate analogue template relative to its enantiomer is better bound by a factor of $K_{M}L/K_{M}D = 0.82$ and 0.79, respectively. The catalytic constant shows the same tendency $k_{cat}L/k_{cat}D$ of 1.36 and 1.22, respectively. As can be seen in Figure 3 the hydrolysis of the control polymer does not show typical Michaelis–Menten kinetics. Therefore, meaningful calculations of k_{cat} and K_M can not be performed.

Table 5. Results of Michaelis–Menten kinetics when the imprinted catalysts **IP4** and **IP5** were used (see Figure 3).

	IP4		IP5	
catalyst substrate	2L	2D	3L	3D
K_M [mM]	0.51	0.62	0.34	0.43
k_{cat} [10^{-4} min^{-1}]	4.74	3.49	3.26	2.68
k_{cat}/K_M [min^{-1}M^{-1}]	0.94	0.57	0.95	0.62
L/D ratio of k_{cat}/K_M	1.66		1.53	

Often k_{cat}/K_M values, a measure of catalytic efficiency, are given for enzymes or enzyme models. If these values are compared to both substrate enantiomers, an enantioselectivity for **IP4** of 1.66 and for **IP5** of 1.53 is obtained. This shows remarkable enantioselectivity for this catalytic action. Furthermore, it shows that the rate enhancement of one enantiomer is caused by the better binding of the template analogue substrate, as well as by a better stabilization of the template analogue transition state of the reaction. Thus, thermodynamic and kinetic influences are observed to a similar extent.

A typical property of enzymes is the inhibition by certain molecules. A transition-state analogue imprinted polymer should show competitive inhibition by the template. This would be a further proof for catalysis to occur inside the imprinted cavity. Figure 4 shows a double-reciprocal Lineweaver–Burk plot for initial reaction rates (v_0^{-1}) versus substrate concentration (c^{-1}). The reactions were run in the

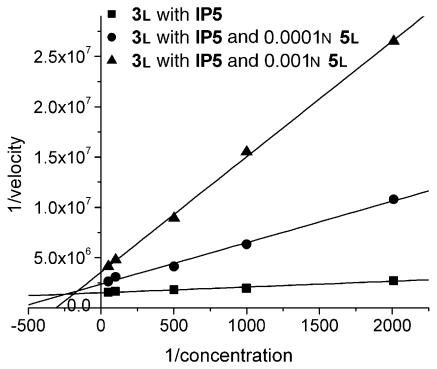

Figure 4. Lineweaver–Burk plot of the kinetics for the hydrolysis of **3L** in acetonitrile/0.1N HEPES buffer pH 7.3 (1:1), in the presence of polymer **IP5** with different inhibitor **5** concentrations.

presence of catalyst **IP5** under standard conditions, firstly without addition of an inhibitor, and secondly with two different concentrations of template **5L**. Evidently, **5L** is a very effective inhibitor that binds much better than the substrate **3L** by a factor of 24 [K_i(competitive) = 0.016 mM]. From the plot in Figure 4, this does not suggest to be pure competitive inhibition. Since the straight lines intersect in the negative part of the plot (and not on the ordinate), a mixed competitive (noncompetitive) inhibition seems to be present (i.e., not only the catalyst, but also the catalyst–substrate complex can bind to the inhibitor). Since the accuracy of the kinetic measurements is not high enough, we have not calculated the different inhibitor constants.

Conclusion

Very active, molecularly-imprinted catalysts with enzyme-like properties were prepared. They showed pronounced substrate- and enantioselectivity. The origin of the enantioselectivity was investigated by determining the plots of initial velocities versus substrate concentration. As a result, the Michaelis constants K_m and the catalytic constants k_{cat} were determined for both enantiomers. The enantioselectivity is caused, to a similar degree, by selective-substrate binding (thermodynamic control), and selective formation of the transition state of the reaction (kinetic control). Strong competitive inhibition by the template (a stable transition-state analogue of the reaction) was observed in the catalysis.

Experimental Section

Instrumentation: Elemental analysis was performed in the microanalytical laboratories of the Faculty of Natural Sciences of the Heinrich-Heine University in Düsseldorf (Perkin–Elmer 2400). ^{1}H (500 MHz) and ^{13}C{^{1}H} NMR (125.8 MHz) spectra were recorded on a Bruker DRX 500, and the ^{31}PNMR (81 MHz) on a Bruker AC 200 with TMS as an internal standard. NMR spectra were measured in $CDCl_3$ at 25 °C if not otherwise stated. Optical rotations were measured with a Perkin–Elmer 241 MC polarimeter (accuracy ± 0.002°). The mass spectra were measured on a Varian MAT 311 A (EI), a Finnigan Mat 8200 (EI), a Finnigan Mat 8200 (FAB with 3-nitrobenzylalcohol (NBA) as matrix, and if required with addition of sodium chloride), or a Finnigan INCOS 50 (CI). All infrared spectra were recorded with a Bruker Vector 22 FT-IR-spectrophotometer. The melting points were measured by using a Büchi Melting Point B-545. The inner surfaces (one point BET-isotherm) were measured by JUWE Laborgeräte GmbH, Viersen (JUWE BET-A-MAT).

Materials: The solvents for HPLC (acetonitrile: isocratic grade), and all solvents for the coupling reactions and polymerisations: methylene chloride (peptide grade), chloroform (dry), methanol (extra dry), toluene (dry), acetonitrile (dry), and ethanol (dry) were supplied from Biosolve. All amino acid reactants (puris.), and the coupling reagent BOP and oxalyl chloride were purchased from Fluka. *N*-Methyl morpholine, terephthalic acid monomethyl ester, and bromotrimethylsilane, trifluoro acetic acid were obtained from Aldrich, and 1,4-dioxane (puriss p.a.), [18]crown-6, and 30% hydrogen bromide in acetic acid were obtained from Merck. 3,5-Dimethyl phenol from Aldrich was further purified by sublimation. Azobisisobutyronitrile from Aldrich was further purified by recrystallization from dry methanol. Ethylene glycol dimethycrylate and methyl methacrylate were purchased from Aldrich, and purified by drying over calcium hydride and distillation. All other solvents were used in distilled grade.

HPLC: All HPLC measurements were performed with a set-up consisting of a Waters 410 pump, a Waters 486 UV-detector, and spectral recording and integration software CSW Chromatography Station for Windows, Version 1.7, 2000, Apex Data Ltd. As columns, a RP-18 ACE-EPS (Bischoff) or a RP-18 (Merck) were used. Acetophenone was used as an internal standard, which was distilled before usage.

General procedure for esterification; example 7D: *N*-Cbz-D-valine (6.68 g, 0.0266 mol) in dry methylene chloride (160 mL) were treated at room temperature with 3,5-dimethyl phenol (3.25 g, 0.0266 mol), BOP (11.76 g, 0.0266 mol), and *N*-methyl morpholine (1.88 mL, 0.0266 mol). After being stirring overnight, the solvent was removed, and the product was purified by column chromatography (chloroform/hexane/acetone 4:10:1). The product was obtained in a yield of 57.5% (5.43g).

***N*-Benzyloxycarbonyl-L-leucine 3,5-dimethylphenyl ester (6L)**: Yield: 39.5%; colorless oil; $[\alpha]_D^{25} = -15.9°$ ($c = 2.0$ in $CHCl_3$); ^{1}H NMR: $\delta = 1.01$ (d, ^3J(H,H) = 5.4 Hz, 3H; CHCH_3), 1.02 (d, ^3J(H,H) = 4.8 Hz, 3H; CHCH_3), 1.67 (m, 1H; $CH_2CH(CH_3)_2$), 1.82 (m, 2H; $CH_2CH(CH_3)_2$), 2.31 (s, 6H; CCH_3), 4.61 (dt, ^3J(H,H) = 4.4, ^3J(H,H) = 8.7 Hz, 1H; NHCHCH$_2$), 5.14 (s, 2H; OCH_2), 5.21 (d, ^3J(H,H) = 8.5 Hz, 1H; NH), 6.69 (s, 2H; ArH), 6.87 (s, 1H; ArH), 7.33 ppm (m, 5H; PhH); ^{13}C NMR: $\delta = 19.8$, 20.5, 21.5, 23.5 (*C*H$_3$), 40.3 (*C*H$_2$), 51.3 (*C*H), 65.7 (*C*H$_2$), 117.4, 126.4, 126.7, 126.8, 127.1 (Ar*C*H), 134.8, 137.9, 148.9 (Ar*C*), 154.6, 170.6 ppm (*C*=O); FT-IR: $\tilde{\nu} = 3339$ (NH), 3034 (Ar-H), 2969 (CH$_3$), 2871 (CH$_2$), 1764 (C=O ester), 1723 (C=O carbamate), 1618 (carbamate), 1529 cm^{-1} (NH); MS (EI): m/z: 369 [M^+]; elemental analysis calcd (%) for $C_{22}H_{27}NO_4$ (369.5): C 71.52, H 7.37, N 3.79; found: C 70.95, H 7.34, N 3.91.

***N*-Benzyloxycarbonyl-D-leucine 3,5-dimethylphenyl ester (6D)**: Yield: 60.8%; colorless oil; $[\alpha]_D^{25} = +16.0°$ ($c = 2.0$ in $CHCl_3$); spectra analogue to **6L**; elemental analysis calcd (%) for $C_{22}H_{27}NO_4$ (369.5): C 71.52, H 7.37, N 3.79; found: C 70.87, H 7.13, N 3.91.

***N*-Benzyloxycarbonyl-L-valine 3,5-dimethylphenyl ester (7L)**: Yield: 98.0%; m.p. 52 °C; $[\alpha]_D^{25} = -11.6°$ ($c = 2.0$ in $CHCl_3$); ^{1}H NMR: $\delta = 1.04$ (d, ^3J(H,H) = 6.7 Hz, 3H; CHCH_3), 1.08 (d, ^3J(H,H) = 6.6 Hz, 3H; CHCH_3), 2.30 (s, 6H; CCH_3), 2.34 (m, 1H; CH(CH$_3$)$_2$), 4.53 (dd, ^3J(H,H) = 4.7, ^3J(H,H) = 9.2 Hz, 1H; NHCHCH), 5.14 (s, 2H, OCH_2), 5.35 (d, ^3J(H,H) = 9.2 Hz, 1H; NH), 6.68 (s, 2H; ArH), 6.87 (s, 1H; ArH), 7.36 ppm (m, 5H; PhH); ^{13}C NMR: $\delta = 18.0$, 19.5, 21.4 (*C*H$_3$), 31.8, 59.6 (*C*H), 67.5 (*C*H$_2$), 119.3, 128.3, 128.6, 129.0, 136.7 (Ar*C*H), 139.8, 150.7, 150.7, 156.7 (Ar*C*), 171.3, 171.5 ppm (*C*=O); FT-IR (KBr): $\tilde{\nu} = 3352$ (NH), 3035 (Ar-H), 2986 (CH$_3$), 2963 (CH$_3$), 1772 (C=O ester), 1693 (C=O carbamate), 1618 (carbamate), 1528 cm^{-1} (NH); MS (EI): m/z: 355 [M^+]; elemental analysis calcd (%) for $C_{21}H_{25}NO_4$ (355.4): C 70.96, H 7.09, N 3.94; found: C 70.98, H 7.28, N 3.89.

***N*-Benzyloxycarbonyl-D-valine 3,5-dimethylphenyl ester (7D)**: Yield: 57.5%; m.p. 54 °C; $[\alpha]_D^{25} = +11.6°$ (c = 2.0 in $CHCl_3$); spectra analogue to **7L**; elemental analysis calcd (%) for $C_{21}H_{25}NO_4$ (355.4): C 70.96, H 7.09, N 3.94; found: C 70.75, H 7.10, N 3.96.

General procedure for deprotection; example for 9L: Ester **7L** (1.50 g, 4.220 mmol) in 30% hydrogen bromide in acetic acid (20 mL) was stirred for 3 h at room temperature. The excess hydrogen bromide in acetic acid was removed by evaporation, and the remaining solid was dried. The product was taken up in dry diethyl ether, filtered off, and washed with a

small amount of dry diethyl ether. The crude product was pure and could further be used directly, and was obtained in a yield of 90.2% (1.15 g).

L-Leucine 3,5-dimethylphenyl ester hydrobromide (8L): Yield: 75.2%; m.p. 213°C; $[\alpha]_D^{25} = +26.3°$ ($c = 2.0$ in MeOH); ^{1}H NMR ([D$_6$]DMSO): $\delta = 0.97$ (d, ^3J(H,H) = 4.8 Hz, 3H; CHCH_3), 0.98 (d, ^3J(H,H) = 4.7 Hz, 3H; CHCH_3), 1.76(m, 1H; CH_2CH(CH$_3$)$_2$), 1.85 (m, 2H; CH_2CH(CH$_3$)$_2$), 2.30 (s, 6H; CCH_3), 4.26 (t, ^3J(H,H) = 6.9 Hz, 1H; NHCHCH$_2$), 6.80 (s, 2H; ArH), 6.97 (s, 1H; ArH), 8.49 ppm (brs, 3H; NH_3); ^{13}C NMR ([D$_6$]DMSO): $\delta = 21.1$, 22.4, 22.5 (CH$_3$), 24.3 (CH), 39.5 (CH$_2$), 51.1 (CH), 119.0, 128.3 (ArCH), 139.6, 150.0 (ArC), 169.2 ppm (C=O); FT-IR (KBr): $\tilde{\nu} = 2952$ (CH$_3$), 1771 (C=O ester), 1591 (NH$_3^+$), 1495 cm^{-1} (NH$_3^+$); MS (FAB, NBA): m/z: 236 [M−Br$^+$]; elemental analysis calcd (%) for C$_{14}$H$_{22}$BrNO$_2$ (316.2): C 53.17, H 7.01, N 4.43; found: C 53.03, H 6.75, N 4.49.

D-Leucine-3,5-dimethylphenyl ester hydrobromide (8D): Yield: 71.9%; m.p. 217°C; $[\alpha]_D^{25} = -26.2°$ [c = 2.0 in MeOH]; spectra analogue to **8L**; elemental analysis calcd (%) for C$_{14}$H$_{22}$BrNO$_2$ (316.2): C 53.17, H 7.01, N 4.43; found: C 53.04, H 6.94, N 4.37.

L-Valine 3,5-dimethylphenyl ester hydrobromide (9L): Yield: 90.2%; m.p. 204°C; $[\alpha]_D^{25} = +19.5°$ ($c = 2.0$ in MeOH); ^{1}H NMR ([D$_6$]DMSO): $\delta = 1.08$ (d, ^3J(H,H) = 7.0 Hz, 3H; CHCH_3), 1.11 (d, ^3J(H,H) = 7.0 Hz, 3H; CHCH_3), 2.30 (s, 6H; CCH_3), 2.35 (m, 1H; CH(CH$_3$)$_2$), 4.20(d, ^3J(H,H) = 4.8 Hz, 1H; NHCHCH), 6.79 (s, 2H; ArH), 6.97 (s, 1H; ArH), 8.51 ppm (brs, 3H; NH_3); ^{13}C NMR ([D$_6$]DMSO): $\delta = 18.1$, 18.7, 21.1 (CH$_3$), 29.9 (CH$_2$), 57.7 (CH), 119.1, 128.4 (ArCH), 139.7, 149.9 (ArC), 168.1 ppm (C=O); FT-IR (KBr): $\tilde{\nu} = 2970$ (CH$_3$), 1753 (C=O ester), 1583 (NH$_3^+$), 1501 cm^{-1} (NH$_3^+$); MS (FAB, NBA): m/z 222 [M−Br$^+$]; elemental analysis calcd (%) for C$_{13}$H$_{20}$BrNO$_2$ (302.2): C 51.67, H 6.67, N 4.63; found: C 51.48, H 6.63, N 4.53.

D-Valine 3,5-dimethylphenyl ester hydrobromide (9D): Yield: 61.3%; m.p. 202°C; $[\alpha]_D^{25} = -19.9°$ ($c = 2.0$ in MeOH); spectra analogue to **9L**; elemental analysis calcd (%) for C$_{13}$H$_{20}$BrNO$_2$ (302.2): C 51.67, H 6.67, N 4.63; found: C 51.34, H 6.46, N 4.67.

General procedure for the coupling to the amide, example for 11L: Ester **8L** (0.80 g, 2.530 mmol) in dry methylene chloride (60 mL) under argon were mixed with terephthalic acid monomethyl ester (0.49 g, 2.530 mmol), PyCloP (1.17 g, 2.783 mmol), and *N*-methyl morpholine (0.77 g, 7.583 mmol). The mixture was stirred overnight at room temperature. The product was purified by column chromatography (chloroform/hexane/acetone 4:2:1 for **12L**, and for **12D** the eluent was chloroform/hexane/acetone 10:4:1), and a yield of 94.5% (1.13 g) was obtained.

***N*-(*O*-Benzylterephthaloyl)-L-leucine-3,5-dimethylphenyl ester (11L)**: Yield: 94.5%; m.p. 108°C; $[\alpha]_D^{25} = +2.5°$ ($c = 2.0$ in CHCl$_3$); ^{1}H NMR: $\delta = 1.06$ (d, ^3J(H,H) = 4.1 Hz, 3H; CHCH_3), 1.07 (d, ^3J(H,H) = 4.1 Hz, 3H; CHCH_3), 1.85 (m, 2H; CH_2CH(CH$_3$)$_2$), 1.96 (m, 1H; CH$_2$CH(CH$_3$)$_2$), 2.31 (s, 6H; CCH_3), 5.06 (m, 1H; NHCHCH$_2$), 5.38 (s, 2H; OCH_2), 6.62 (d, ^3J(H,H) = 8.2 Hz, 1H, NH), 6.72 (s, 2H; ArH), 6.88 (s, 1H; ArH), 7.40 (m, 5H; PhH), 7.87 (d, ^3J(H,H) = 8.5 Hz, 2H; ArH), 8.14 ppm (d, ^3J(H,H) = 8.4 Hz, 2H; ArH); ^{13}C NMR: $\delta = 21.2$, 22.1, 22.9 (CH$_3$), 25.2 (CH), 41.8 (CH$_2$), 51.5 (CH), 67.1 (CH$_2$), 118.8, 127.2, 128.0, 128.3, 128.4, 128.7, 130.0 (ArCH), 133.0, 135.7, 137.9, 139.5, 150.3 (ArC), 165.6, 166.4, 171.9 ppm (C=O); FT-IR (KBr, cm^{-1}): $\tilde{\nu} = 3260$ (NH), 2957 (CH$_3$), 1762 (C=O ester), 1722 (C=O ester), 1638 (C=O amide), 1538 (amide); MS (EI): m/z: 473 [M^+]; elemental analysis calcd (%) C$_{29}$H$_{31}$NO$_5$ (473.6): C 73.55, H 6.60, N 2.96; found: C 73.28, H 6.56, N 3.06.

***N*-(*O*-Benzylterephthaloyl)-D-leucine-3,5-dimethylphenyl ester (11D)**: Yield: 92.3%; m.p. 108°C; $[\alpha]_D^{25} = -2.5°$ (c = 2.0 in CHCl$_3$)]; spectra analogue to **11L**; elemental analysis calcd (%) for C$_{29}$H$_{31}$NO$_5$ (473.6): C 73.55, H 6.60, N 2.96; found: C 73.65, H 6.88 , N 3.10.

***N*-(*O*-Benzylterephthaloyl)-L-valine-3,5-dimethylphenyl ester (12L)**: Yield: 78.0%; m.p. 106°C; $[\alpha]_D^{25} = +10.8°$ (c = 2.0 in CHCl$_3$); ^{1}H NMR: $\delta = 1.29$ (d, ^3J(H,H) = 7.0 Hz, 3H; CHCH_3), 1.14 (d, ^3J(H,H) = 7.3 Hz, 3H; CHCH_3), 2.32 (s, 6H; CCH_3), 2.48 (m, 1H; CH(CH$_3$)$_2$), 5.01 (dd, ^3J(H,H) = 4.8, ^3J(H,H) = 8.5 Hz, 1H; NHCHCH), 5.39 (s, 2H; OCH_2), 6.70 (d, ^3J(H,H) = 8.8 Hz, 1H; NH), 6.71 (s, 2H; ArH), 6.89 (s, 1H; ArH), 7.36 (m, 5H; PhH), 7.88 (d, ^3J(H,H) = 8.9 Hz, 2H; ArH), 7.88 ppm (d, ^3J(H,H) = 8.4 Hz, 2H; ArH); ^{13}C NMR: $\delta = 18.1$, 19.1, 21.2 (CH$_3$), 21.8, 57.7 (CH), 67.1 (CH$_2$), 118.8, 127.2, 128.0, 128.3, 128.4, 128.7, 130.1 (ArCH), 133.0, 135.7, 138.1, 139.5, 150.2 (ArC), 165.6, 166.6, 170.9 ppm (C=O); FT-IR (KBr): $\tilde{\nu}$ = 3299 (NH), 2973 (CH$_3$), 1756 (C=O ester), 1724 (C=O ester), 1642 (C=O amide), 1542 cm^{-1} (amide); MS (FAB, NBA): m/z: 460 [M^++H]; elemental analysis calcd (%) for C$_{28}$H$_{29}$NO$_5$ (459.5): C 73.18, H 6.36, N 3.05; found: C 72.84, H 6.38, N 3.22.

***N*-(*O*-Benzylterephthaloyl)-D-valine 3,5-dimethylphenyl ester (12D)**: Yield: 78.0%; m.p. 106°C; $[\alpha]_D^{25} = -10.9°$ (c = 2.0 in CHCl$_3$); spectra analogue to **12L**; elemental analysis calcd (%) for C$_{28}$H$_{29}$NO$_5$ (459.5): C 73.18, H 6.36, N 3.05; found: C 72.96, H 6.34, N 3.09.

General procedure for the hydrogenation, example for 2L: Palladium hydroxide on carbon (0.50 g) was added to **11L** (1.20 g, 2.53 mmol) in ethanol (60 mL), and treated with hydrogen gas (1 bar). After 2 to 3 days the catalyst was filtered off over celite (reaction was followed by TLC). The solvent was removed, and the obtained crude product was purified by column chromatography (ethyl acetate with 1% acetic acid/methanol 3:1). To remove the acetic acid completely, the product was dried over potassium hydroxide. The product was recrystallized from cyclohexane and dry ethanol, and a yield of 91.1% (0.88 g) was obtained.

***N*-Terephthaloyl-L-leucin 3,5-dimethylphenylester (2L)**: Yield: 91.1%; m.p. 162°C; $[\alpha]_D^{25} = -6.6°$ (c = 2.0 in CHCl$_3$); ^{1}H NMR: $\delta = 1{,}07$ (d, ^3J(H,H) = 1.6 Hz, 3H; CHCH_3), 1.08 (d, ^3J(H,H) = 1.9 Hz, 3H; CHCH_3), 1.87 (m, 2H; CH_2CH(CH$_3$)$_2$), 1.73 (m, 1H; CH$_2$CH(CH$_3$)$_2$), 2.32 (s, 6H; CCH_3), 5.08 (m, 1H; NHCHCH$_2$), 6.74 (s, 2H; ArH), 6,74 (d, ^3J(H,H) = 7.3 Hz, 1H; NH), 6.89 (s, 1H; ArH), 7.88 (d, ^3J(H,H) = 8.5 Hz, 2H; ArH), 8.12 ppm (d, ^3J(H,H) = 8.2 Hz, 2H; ArH); ^{13}C NMR: $\delta = 21.2$, 22.1 (CH$_3$), 22.9 (CH), 25.2, 25.2 (CH$_3$), 41.7 (CH$_2$), 51.6 (CH), 118.8, 127.3, 128.0, 130.5 (ArCH), 132.1, 138.5, 139.5, 150.3 (ArC), 166.6, 169.9, 172.3 ppm (C=O); FT-IR (KBr): $\tilde{\nu} = 3356$ (NH), 2960 (CH$_3$), 1752 (C=O ester), 1701 (COOH), 1641 (C=O amide), 1528 cm^{-1} (amide); MS (FAB, NBA): m/z 406 ([M$^+$+Na]), 384 ([M$^+$+H]); elemental analysis calcd (%) for C$_{22}$H$_{25}$NO$_5$·0.5H$_2$O (383.4 + 9.0): C 67.33, H 6.68, N 3.57; found: C 67.04, H 6.66, N 3.48.

***N*-Terephthaloyl-D-leucine 3,5-dimethylphenyl ester (2D)**: Yield: 94.8%; m.p. 162°C; $[\alpha]_D^{25} = +6.6°$ (c = 2.0 in CHCl$_3$); spectra analogue to **2L**; elemental analysis calcd (%) for C$_{22}$H$_{25}$NO$_5$ (383.4): C 68.91, H 6.57, N 3.65; found: C 68.75, H 6.71, N 3.76.

***N*-Terephthaloyl-L-valine 3,5-dimethylphenyl ester (3L)**: Yield: 87.8%; m.p. 153°C; $[\alpha]_D^{25} = +6.7°$ (c = 2.0 in CHCl$_3$); ^{1}H NMR: $\delta = 1.18$ (d, ^3J(H,H) = 2.5 Hz, 3H; CHCH_3), 1.22 (^3J(H,H) = 2.5 Hz, 3H; CHCH_3), 2.37 (s, 6H; CCH_3), 2.55 (m, 1H; CH(CH$_3$)$_2$), 5.07 (dd, ^3J(H,H) = 4.8, ^3J(H,H) = 8.8 Hz, 1H; NHCHCH), 6.77 (s, 2H, ArH), 6,88 (d, ^3J(H,H) = 8.8 Hz, 1H; NH), 6.94 (s, 1H; ArH), 7.93 (d, ^3J(H,H) = 8.5 Hz, 2H; ArH), 8.19 ppm (d, ^3J(H,H) = 8.5 Hz, 2H; ArH); ^{13}C NMR: $\delta = 18.1$, 19.2, 21.2 (CH$_3$), 31.7, 57.7 (CH), 118.8, 127.3, 128.1, 130.5 (ArCH), 132.1, 138.7, 139.5, 150.2 (ArC), 166.8, 170.0, 171.2 ppm (C=O); FT-IR (KBr): $\tilde{\nu} = 3345$ (NH), 2968 (CH$_3$), 1756 (C=O ester), 1681 (COOH), 1644 (C=O amide), 1531 cm^{-1} (amide); MS (FAB, NBA): m/z 392 ([M$^+$+Na]), 370 ([M$^+$+H]); elemental analysis calcd (%) for C$_{21}$H$_{23}$NO$_5$·0.25H$_2$O (369.4 + 4.5): C 67.46, H 6.33, N 3.75; found: C 67.38, H 6.51, N 3.61.

***N*-Terephthaloyl-D-valine 3,5-dimethylphenyl ester (3D)**: Yield: 93.3%; m.p. 153°C; $[\alpha]_D^{25} = -6.6°$ (c = 2.0 in CHCl$_3$); spectra analogue to **3L**; elemental analysis calcd (%) for C$_{21}$H$_{23}$NO$_5$·0.5H$_2$O (369.4 + 9,0): C 66.65, H 6.39, N 3.70; found: C 66.51, H 6.47, N 3.75.

General procedure for coupling of the amide to 17: The α-L-aminophosphonic acid **14**[22] (5.19 g, 0.0247 mol) in dry methylene chloride (180 mL) under an argon atmosphere were treated with PyCloP (10.41 g, 0.0247 mol), *N*-methyl morpholine (5.00 g, 0.0494 mol), and monomethyl terephthalate (**15**) (4.45 g, 0.0247 mol); the mixture was stirred for 48 h at room temperature. The solvent was then evaporated, and the product was purified by column chromatography in chloroform/hexane/acetone 4:1:1 to give a yield of 87.5% (8.03 g).

L-*N*-[1-(Diethoxyphosphoryl)-3-methylbutyl]terephthalamic acid methyl ester (16): Yield: 90.5%; colorless oil; $[\alpha]_D^{25} = -10{,}8°$ [c = 2.0 in CHCl$_3$]; ^{1}H NMR: $\delta = 0.96$ (s, 3H; CHCH_3), 0.99 (s, 3H; CHCH_3), 1.22 (t, ^3J(H,H) = 7.0 Hz, 3H; CH$_2$CH_3), 1.36 (t, ^3J(H,H) = 7.2 Hz, 3H; CH$_2$CH_3), 1.77 (m, 3H; CH_2CH(CH$_3$)$_2$), 3.94 (s, 3H; OCH$_3$), 4.11 (m, 4H; CH$_2$CH$_3$), 4.79 (m, 1H; NHCHP), 7.33 (d, ^3J(H,H) = 11.0 Hz, 1H; NH), 7.92 (d, ^3J(H,H) = 8.5 Hz, 2H; ArH), 8.10 ppm (d, ^3J(H,H) = 8.5 Hz, 2H; ArH); ^{13}C NMR: $\delta = 16.8$ (d), 17.0 (d) (Et−CH$_3$), 21.7, 22.1 (CH$_3$), 24.5 (d) (CH), 38.6 (CH$_2$), 44.5 (d) (CH$_2$), 52.8 (OCH$_3$), 62.8 (d), 63.2 (d) (OCH$_2$), 127.8, 130.0 (ArCH), 133.1, 138.4 (ArC), 166.6, 166.6 ppm (C=O); ^{31}P NMR (81 MHz, CDCl$_3$): $\delta = 26.3$ (s); FT-IR (cm^{-1}): $\tilde{\nu} = 3267$ (NH), 2957 (CH$_3$), 2871 (CH$_2$), 1728 (C=O ester) 1661 (C=O amide), 1542 (amide), 1280

(P=O), 1031 (P–O–C); MS (EI): m/z 385 (M^+); elemental analysis calcd (%) for $C_{18}H_{28}NO_6P \cdot 0.25H_2O$ (385.4 + 4.5): C 55.45, H 7.37, N 3.59; found: C 55.56, H 7.50, N 3.69.

L-*N*-[1-(Diethoxyphosphoryl)-2-methylpropyl]terephthalamic acid methyl ester (17): Yield: 87.5%; m.p. 81 °C; $[\alpha]_D^{25} = -2.5°$ (c = 2.0 in $CHCl_3$); ^{1}H NMR: $\delta = 1.11$ (dd, ^3J(H,H) = 6.8, ^4J(P,H) = 1.3 Hz, 3H; CHCH_3), 1.12 (d, ^3J(H,H) = 6.8 Hz, 3H; CHCH_3), 1.27 (t, ^3J(H,H) = 7.5 Hz, 3H; CH_2CH_3), 1.37(t, ^3J(H,H) = 7.0 Hz, 3H; CH_2CH_3), 2.35 (m, 4H; CH(CH_3)$_2$), 3.98 (s, 3H; OCH_3), 4.14 (m, 3H; CH_2CH$_3$), 4.62 (ddd, ^3J(H,H) = 4.8 Hz, ^3J(H,H) = 10.4 Hz, ^2J(P,H) = 18.1 Hz, 1H; NHCHP), 6.72 (dd, ^3J(H,H) = 10.4 Hz, ^3J(P,H) = 2.6 Hz, 1H; NH), 7.90 (d, ^3J(H,H) = 8.8 Hz, 2H; ArH), 8.14 ppm (d, ^3J(H,H) = 8.8 Hz, 2H; ArH); ^{13}C{^{1}H} NMR: $\delta = 16.8$ (d), 18.2 (d) (Et–CH_3), 20.6 (d) (CH_3), 29.3 (d), 50.8 (d) (CH), 52.8 (OCH_3), 62.5 (d), 62.6 (d) (OCH_2), 127.1 (d), 129.9 (d), (ArCH), 133.0, 138.0 (ArC), 166.2, 166.6 ppm (d) (C=O); ^{31}P NMR: δ = 25.2 (s); FT-IR (KBr): $\tilde{\nu} = 3261$ (NH), 2981 (CH_3), 1725 (C=O ester) 1659 (C=O amide), 1544 (amide), 1278 (P=O), 1031 cm^{-1} (P–O–C); MS (CI, NH_3): m/z 370 ([M+H]$^+$), 371 (M^+); elemental analysis calcd (%) for $C_{17}H_{26}NO_6P$ (371.4): C 54.98, H 7.06, N 3.77; found: C 54.82, H 7.19, N 3.81.

General procedure for the hydrolysis, chlorination, and esterification of the P-terminal part to produce 19: Bromo trimethylsilane (4.27 g, 0.0337 mol) was added in batches to **17** (0.50 g, 6.73 mmol) in dry methylene chloride (60 mL) under an argon atmosphere. After the mixture was stirred for 14 h at room temperature, the solution was evaporated, and THF (20 mL) and water (2 mL) were added. After an additional 5 h, the solution was again evaporated and dried by oil pump vacuum (0.05 mbar). The obtained crude product was used without further purification. Some drops of DMF were added to the hydrolysis product in dry methylene chloride (60 mL) under argon oxalyl chloride (5.13 g, 0.0404 mol) for activation. After the mixture was stirred for 11 h, the solvent and the excess oxalyl chloride were removed, and the product was dried under an oil pump vacuum (0.05 mbar). The crude product was used without further purification. After chlorination, the residue in dry methylene chloride (60 mL) under an argon atmosphere was treated with 3,5-dimethylphenol (1.73 g, 0.0141 mol) and *N*-methyl morpholine (1.43 g, 0.0141 mol); it was then stirred for 13 h at room temperature. After evaporation, the product was purified by column chromatography (hexane/chloroform/acetone 10:4:1). The product obtained was in a yield of 47.4% (1.67 g) over 3 steps, and was used directly because of its instability towards oxidation.

L-*N*-{1-[Bis-(3,5-dimethylphenoxy)phosphoryl]-3-methylbutyl}terephthalamic acid methyl ester (18): Yield: 57.3% over 3 steps; colorless oil; ^{1}H NMR: $\delta = 1.03$ (d, ^3J(H,H) = 5.8 Hz, 3H; CHCH_3), 1.06 (d, ^3J(H,H) = 6.0 Hz, 3H; CHCH_3), 1.88 (m, 3H; CH_2CH(CH$_3$)$_2$), 2.15 (s, 6H; CCH_3), 3.99 (s, 3H; OCH_3), 5.17 (m, 1H; NHCHP), 6.62 (br dd, 1H; NH), 6.79 (3s, 6H; ArH), 7.75(d, ^3J(H,H) = 8.3 Hz, 2H; ArH), 8.05 ppm (d,^3J(H,H) = 8.5 Hz, 2H; ArH); ^{13}C NMR: $\delta = 18.5$, 18.6, 20.9 (d), 21.4 (CH_3), 26.5 (d) (CH_2), 41.1 (CH), 51.7 (OCH3), 52.9 (CH), 113.5, 118.3, 122.7, 127.4, 127.7 (d), 130.2 (ArCH), 133.4, 137.8, 139.9 (d), 140.2, 150.4 (ArC), 166.7, 167.2 ppm (d) (C=O); ^{31}P NMR: $\delta = 18.4$ ppm (s); FT-IR (cm^{-1}): $\tilde{\nu} = 3279$ (NH), 3018 (Ar-H), 2962 (CH_3), 2921 (CH_3), 2875 (CH), 1737 (C=O ester), 1669 (C=O amide), 1536 (amide), 1280 (P=O), 1030 (P–O–C); MS (EI): *m/z*: 402 ([M – 135$^+$]$^?$); elemental analysis calcd (%) for $C_{30}H_{36}NO_6P$ (537.6): C 67.03, H 6.75, N 2.61; found: C 67.22 , H 6.72, N 2.57.

L-*N*-{1-[Bis-(3,5-dimethylphenoxy)phosphoryl]-3-methylpropyl}terephthalamic acid methyl ester (19): Yield: 47.4% over 3 steps; colorless oil; ^{1}H NMR: $\delta = 1.21$ (dd, ^3J(H,H) = 6.8, ^4J(P,H) = 1.4 Hz, 3H; CHCH_3), 1.23 (d, ^3J(H,H) = 6.9 Hz, 3H; CHCH_3), 2.11 (s, 6H; CCH_3), 2.34 (s, 6H; CCH_3), 2.55 (m, 1H; CH(CH$_3$)$_2$), 4.00 (s, 3H; OCH_3), 5.10 (ddd, ^3J(H,H) = 4.8, ^3J(H,H) = 10.4, ^2J(P,H) = 19.4 Hz, 1H; NHCHP), 6.72 (m, 4H; ArH), 6.91 (m, 2H; ArH), 7.77 (d, ^3J(H,H) = 8.8 Hz, 2H; ArH), 8.07 ppm (d, ^3J(H,H) = 8.8 Hz, 2H; ArH); ^{13}C NMR: $\delta = 18.5$, 18.6, 20.9 (d), 21.4 (CH_3), 30.1 (d) (CH), 51.7 (OCH3), 52.9 (CH), 113.5, 118.3, 122.7, 127.4, 127.7 (d), 130.2 (ArCH), 133.4, 137.8, 139.9 (d), 140.2, 150.4 (ArC), 166.7, 167.2 ppm (d, C=O); ^{31}P NMR (81 MHz, $CHCl_3$): $\delta = 17.7$ ppm (s); FT-IR: $\tilde{\nu} = 3289$ (NH), 3018 (Ar–H), 2965 (CH_3), 2922 (CH_3), 2875 (CH), 1729 (C=O ester), 1668 (C=O amide), 1538 (amide), 1279 (P=O), 1031 cm^{-1}(P–O–C); MS (CI, NH_3 , 200 °C): *m/z*: 524 ([M$^+$+H]), 541 ([M$^+$+NH_4]); elemental analysis calcd (%) for $C_{29}H_{34}NO_5P$ (523.6): C 66.53, H 6.55, N 2.68; found: C 66.23, H 6.58, N 2.58.

General procedure for the combined hydrolysis to produce 5L: Compound **19** (1.00 g, 1.91 mmol) suspended in 1,4-dioxane (10 mL) and water (10 mL), was treated with [18]crown-6 (30 mg), and a 1N sodium hydroxide solution (3.82 mL, 3.82 mmol). After the mixtures was stirred for 12 h at room temperature, the solution was evaporated and dried. The product was purified by means of column chromatography with a solvent mixture of chloroform and ammoniacal methanol (10% NH_3 in MeOH) in the ratio 3:1, and was then transformed in the dipotassium salt by an ion exchange column loaded with potassium ions. This produced a yield of 76.2% (0.59 g).

Dipotassium salt of *N*-(4-carboxybenzoyl)-1-L-amino-3-methylbutylphosphonic acid-3,5-dimethylphenyl ester (4L): Yield: 72.5%; m.p. decomposition > 280 °C; $[\alpha]_D^{25} = +7.2°$ (c = 2.0 in MeOH); ^{1}H NMR ([D$_6$]DMSO): $\delta = 0.88$ (d, ^3J(H,H) = 4.0 Hz, 6H; CHCH_3), 1.60 (m, 3H; CH_2CH(CH$_3$)$_2$), 2.12 (s, 6H; CCH_3), 4.22 (m, 1H; NHCHP), 6.51 (s, 2H; ArH), 6.67 (s, 1H; ArH), 7.59 (dd, ^3J(H,H) = 9.5 Hz, ^4J(P,H) = 2.8, 1H; NH), 7.77 (d, ^3J(H,H) = 8.3 Hz, ArH), 7.84 ppm (d, ^3J(H,H) = 8.0 Hz, 2H; ArH); ^{13}C NMR: $\delta = 21.7$ (d), 22.3 (CH_3), 24.5 (CH), 26.5 (d) (CH_2), 41.1 (CH), 120.0 (d), 126.2, 128.2, 130.6 (ArCH), 137.6, 140.2, 142.5, 149.3, 155.1 (ArC), 169.5, 174.6 (C=O); ^{31}P NMR ([D$_6$]DMSO)): $\delta = 15.6$ (s); FT-IR (KBr): $\tilde{\nu} = 3384$ (NH), 2957 (CH_3), 1626 (C=O amide), 1595 (COO$^-$), 1559 (amide), 1420 (COO$^-$), 1208 cm^{-1} (P=O);; MS (FAB, NBA): m/z 464 ([M+H]$^?$), 486 ([M+Na]$^?$); elemental analysis calcd (%) for $C_{21}H_{24}NO_6PK_2 \cdot 1\,H_2O$(463.59 + 18,0): C 49.11, H 5.10, N 2.73; found: C 49.27, H 4.82, N 2.76.

Dipotassium salt *N*-(4-carboxybenzoyl)-1-L-amino-2-methylpropylphosphonic acid 3,5-dimethylphenyl ester (5L): Yield: 76.2%; m.p. (decomp) > 200 °C; $[\alpha]_D^{25} = +19.7°$ [c = 2.0 in MeOH]; ^{1}H NMR ([D$_6$]DMSO): δ = 0.93 (d, ^3J(H,H) = 6.8 Hz, 3H; CHCH_3), 0.98 (d, ^3J(H,H) = 6.8 Hz, 3H; CHCH_3), 1.25 (m, 1H; CH(CH$_3$)$_2$), 2.09 (s, 6H; CCH_3), 3.99 (ddd, ^3J(H,H) = 4.2, ^3J(H,H) = 9.5, ^2J(P,H) = 17.2 Hz, 1H; NHCHP), 6.49 (s, 1H; ArH), 6,62 (s, 2H; ArH), 7.62 (d, ^3J(H,H) = 8.3 Hz, 2H; ArH), 7.85 (d,^3J(P,H) = 8.3 Hz, 2H; ArH); ^{13}C NMR ([D$_6$]DMSO): $\delta = 19.1$, 21.2, 21.6 (d) (CH_3), 29.9 (CH), 63.2 (d) (CH), 118.8 (d), 123.6, 126.6, 129.2 (ArCH), 136.4, 137.8, 138.0, 154.1 (ArC), 166.3, 172.0 (C=O); ^{31}P NMR ([D$_6$]DMSO): $\delta = 14.1$ (s); FT-IR (KBr): $\tilde{\nu} = 3428$ (NH), 2960 (CH_3), 1634 (C=O amide), 1594 (COO$^-$), 1554 (amide), 1385 (COO$^-$), 1222 (P=O), 1034 cm^{-1} (P–O–C); MS (FAB, NBA): *m/z*: 404 ([M – 2 K + H$^+$]); elemental analysis calcd (%) for $C_{20}H_{22}NO_6PK_2 \cdot 4\,H_2O$ (449.57 + 72.1): C 43.39, H 5.46, N 2.53; found: C 43.43, H 5.21, N 2.70.

Preparation of the imprinted polymers: The binding site monomer *N*,*N*′-diethyl-4-vinylbenzamidine was used in the form of amidinium chloride salt **1** × HCl.[28] One equivalent of template **4L** or **5L**, was dissolved together with two equivalents of the amidine **1**·HCl in dry methanol to form the polymerisable 1:2 complex. The remaining potassium chloride precipitates were removed by membrane filtration. The solution was evaporated, and the dried complex was dissolved in 82% (w/v) ethylene glycol dimethylacrylate (EDMA), 15% (w/v) methyl methacrylate (MMA) in 10 mL acetonitrile/toluene 1:1. The mixtures were homogenized in an ultrasonic bath at a maximum temperature of 40 °C. Finally, the initiator azobisisobutyronitrile (AIBN) was added, and the monomer mixture was degassed by a "freeze-and-thaw" procedure. The polymerization was carried out in bulk at 60 °C for 72 h in an evacuated ampoule. The polymers were crushed and sieved, and only the fraction from 45 to 125 μm was used for the measurements.

To remove the template, the polymer was first swollen in acetonitrile, and after one hour the template was washed out by stirring three to five times in a 1:1 mixture of 0.1M sodium hydroxide and methanol in an ice bath, until no template was present. The amount of released template was controlled by HPLC (eluent: 0.2% (v/v) trifluoroacetic acid/acetonitrile 65:35 (v/v), internal standard acetophenone, flow rate 1 mL min^{-1}). A calibration curve for the determination of the template in the presence of the internal standard acetophenone was established. At the time when no template was detectable, the polymer was washed with water and methanol. Before use, all polymers were dried over phosphorous pentoxide in an vacuum oven at 40 °C.

The polymers were characterized by measuring the inner surface (BET-isotherm), and the amount of active amidine groups that were carried out by acid-base titration. For titration in 11 vials for each, the same amount of polymer (20 mg) as suspended in a 1:1 mixture of a 1M solution of sodium chloride and 1,4-dioxane (10 mL) was used. An increasing amount of HCl

was added until all theoretically present amidine groups were protonated. After the mixture was stirred overnight, an aliquot of 500 μL was taken, and, after removing the polymer by membrane filtration, the solution was transferred in a small plastic vial to measure the pH value (pH-microelectrode, Schott). The resulting curve from the measured pH-value plotted versus the HCl concentration had an inflection point, from which, the amount of accessible amidine-groups could be calculated.

General procedure for the kinetic measurements: The hydrolysis of the esters were carried out at optimal conditions for amidine based polymers in an 1:1 mixture of a 2-[4-(2-hydroxyethyl)-1-piperazino]ethanesulfonic acid (HEPES) buffer, pH 7.3, and acetonitrile at a temperature of 20 °C.[17] For this purpose, dry polymer with free cavities (6×10^{-6} mol; 1.2×10^{-5} mol amidine groups), was dispersed in a 3 mL screw-capped, in the buffer mixture (2.7 mL), which included 30 μL of an 0.05 M internal standard solution (acetophenone in acetonitrile). This gave a 2 mM concentration of free cavities. The polymer was stirred in this solution overnight to swell the polymer, and equilibrate all amidine groups inside. To start the reaction, a freshly prepared substrate solution in acetonitrile (30 μL, 0.1 M, 3×10^{-6} mol) was added to get a final substrate concentration of 1 mM. The hydrolysis of both enantiomers was determined separately at all times to check for enantioselectivity.

In the case of the control experiments, same amounts of dry control polymer and amidine groups were used (1.2×10^{-5} mol). Without the presence of a polymer catalyst, the hydrolysis reactions in solution were carried out in the same solution mixture at the same substrate concentrations.

For each condition the reaction was performed two to three times to reduce measurement errors. During the reactions, six to nine aliquots of 150 μL were taken, the polymer was filtered off through a membrane, and the sample was then collected in an Eppendorf vessel and frozen in liquid nitrogen to stop the reaction. All samples from the reaction with imprinted polymers were taken within four hours, within three days for the control polymers, and within two weeks for the control solution (with no polymer presence). Afterwards each sample was defrosted to room temperature and measured by injecting 20 μL in the HPLC-system. For the mobile phase, acetonitrile, and trifluoroacetic acid (0.2 % v/v) in water 30:70 (v/v) with a flow rate of 1 mL min^{-1} were used, and for the stationary phase, a RP-18 column (Merck) was used. The chosen wavelength corresponded to the absorption of 3,5-dimethyl phenol with λ_{max} 218 nm, which is optimal to detect the product of the reaction. The system was optimized to control the product peak and the internal standard. A detection software package was used to record and integrate the chromatograms.

A calibration curve for the determination of the product phenol in presence of the internal standard acetophenone was established. With this calibration a conversion up to 20 % of the investigated hydrolysis could easily be followed.

Due to the experimental circumstances at the beginning of all the measurements, a small amount of the reaction product was already present. Thus the product concentration, and the total substrate concentration of all data were corrected by a factor of 0.994; this meant, that on average, 0.6 % of the substrate had already been hydrolyzed at the start of the reaction.

The calculations of the reaction rate constants were performed with a linear fit by Origin 7.0. (See Tables 6, 7, and 8)

Michaelis – Menten kinetics: For the imprinted polymers **IP4** and **IP5**, and for the control polymer **CPF**, plots of initial velocities of the catalyzed hydrolysis versus substrate concentration were measured. For these investigations the initial reaction rates were monitored at constant concentration of active sites, and increasing substrate concentration. We chose six different substrate concentrations in Table 9 and five in Table 10. The procedure to measure the velocity was analogous to pseudo-first-order kinetics, as previously described.

Table 6. Reaction rate constants for the hydrolysis of substrates **2L** and **2D** in acetonitrile/HEPES buffer pH 7.3 (1:1) at 20 °C, by using **IP4** and the controls **CPF**, **CPB** and solution in two different buffer concentrations.

Catalyst	Substrate	0.10 M HEPES buffer k [min^{-1}]	0.15 M HEPES buffer k [min^{-1}]
IP4	**2L**[a]	$8.27 \times 10^{-4} \pm 8.5\,\%$	6.69×10^{-4}
IP4	**2D**	$5.95 \times 10^{-4} \pm 2.4\,\%$	5.57×10^{-4}
CPF	**2L**	$1.00 \times 10^{-5} \pm 1.5\,\%$	1.01×10^{-5}
CPF	**2D**	$1.08 \times 10^{-5} \pm 3.4\,\%$	9.84×10^{-6}
average **CPF**	**2**	$1.05 \times 10^{-5} \pm 3.5\,\%$	$9.97 \times 10^{-6} \pm 1.2\,\%$
CPB	**2L**	6.11×10^{-5}	–
CPB	**2D**	5.97×10^{-5}	–
average **CPB**	**2**	$6.04 \times 10^{-5} \pm 1.2\,\%$	–
solution	**2L**	$2.53 \times 10^{-6} \pm 3.8\,\%$	$3.28 \times 10^{-6} \pm 1.7\,\%$
solution	**2D**	$2.56 \times 10^{-6} \pm 7.3\,\%$	$3.42 \times 10^{-6} \pm 9.8\,\%$
average solution	**2**	$2.54 \times 10^{-6} \pm 5.9\,\%$	$3.35 \times 10^{-6} \pm 7.5\,\%$

[a] **2L** = L-leucine substrate; **2D** = D-substrate; **IP4** = polymer imprinted with template **4; CPF** = control polymer imprinted with formic acid; **CPB** = control polymer imprinted with benzoic acid; Solution = acetonitrile/buffer (1:1). When a measurement error is given, the value is investigated two to three times; errors denote standard deviation.

Table 7. Reaction rate constants for the hydrolysis of the substrates **3L** and **3D** using **IP5** and the controls **CPF** and solution. All experiments were performed in acetonitrile/0.1 M HEPES buffer pH 7.3 (1:1).

	substrate	k [min^{-1}]
IP5	**3L**[a]	$5.54 \times 10^{-4} \pm 2.7\,\%$
IP5	**3D**	$4.53 \times 10^{-4} \pm 6.2\,\%$
CPF	**3L**	$9.02 \times 10^{-6} \pm 2.2\,\%$
CPF	**3D**	$9.44 \times 10^{-6} \pm 0.8\,\%$
average **CPF**	**3**	$9.23 \times 10^{-6} \pm 2.8\,\%$
solution	**3L**	$2.16 \times 10^{-6} \pm 1.1\,\%$
solution	**3D**	$2.23 \times 10^{-6} \pm 3.0\,\%$
average solution	**3**	$2.20 \times 10^{-6} \pm 2.6\,\%$

[a] **3L** = L-valine substrate; **3D** = D-substrate; **IP5** = polymer imprinted with template **5; CPF** = control polymer imprinted with formic acid; solution = acetonitrile/buffer (1:1). When a measurement error is given, the value was investigated twice, except for **IP5**, which was investigated three times.

Table 8. Reaction rate constants for cross-selectivity of valine substrate **3L** with polymer **IP4** (leucine-analogue polymer), and leucine substrate **2L**[a] with **IP5** (valine-analogue polymer) in acetonitrile/0.1 M HEPES buffer pH 7.3 (1:1) at 20 °C.

Catalyst	Substrate	k [$\times 10^{-4}$ min^{-1}]
IP4	**3L**	$2.26 \pm 4.1\,\%$
IP5	**2L**	$2.00 \pm 3.1\,\%$

[a] **2L** = L-leucine substrate; **3L** = L-valine substrate.

Table 9. Data of Michaelis – Menten kinetics with **IP4** and **CPF**.[a]

Substrate concentration [mmol L^{-1}]	**2L** with **IP4** v_0 [10^{-7} M min^{-1}]	**2D** with **IP4** v_0 [10^{-7} M min^{-1}]	**2L** with **CPF** v_0 [10^{-8} M min^{-1}]	**2D** with **CPF** v_0 [10^{-8} M min^{-1}]
0.124	2.05	–	–	–
0.497	3.94	2.24	0.61	0.62
0.994	6.99	5.09	0.94	0.10
1.988	7.65	5.62	1.45	1.47
9.940	8.88	6.20	2.04	2.08
19.88	9.19	6.81	2.02	2.06

[a] Reaction velocities obtained by increasing substrate concentration of substrates **2L** and **2D** in acetonitrile/0.1 M HEPES buffer pH 7.3 (1:1) at 20 °C.

Table 10. Data of Michaelis–Menten kinetics with **IP5** without and with two concentration of inhibitor **5L**.[a]

Substrate concentration [mmol L^{-1}]	**3L** with **IP5** v_0 [10^{-} M min^{-1}]	**3D** with **IP5** v_0 [10^{-7} M min^{-1}]	**3L** with **IP5** [I] = 0.0001 M v_0 [10^{-8} M min^{-1}]	**3L** with **IP5** [I] = 0.001 M v_0 [10^{-8} M min^{-1}]
0.497	3.67	2.95	9.25	0.38
0.994	5.10	3.71	1.58	0.65
1.988	5.58	4.34	2.43	1.12
9.940	6.09	5.05	3.25	2.09
19.88	6.51	5.38	3.80	2.43

[a] Reaction velocities obtained by increasing the substrate concentration of substrates **3L** and **3D** in acetonitrile/0.1 M HEPES buffer pH 7.3 (1:1) at 20 °C. [I] = concentration of inhibitor **5L**.

In addition, the influence of the inhibiting molecule template **5**, was monitored with polymer **IP5**. Two different inhibitor concentrations were added to the hydrolysis media to reach the concentration of 1 mM and 0.1 mM. The velocities were monitored in the same way. The obtained results are listed in Tables 9 and 10.

The calculations of the Michaelis–Menten kinetics were performed by fitting them to a hyperbola by the program Origin 7.0.

Acknowledgement

This work was supported by Deutsche Forschungsgemeinschaft, Fonds der Chemischen Industrie, and by the Graduierten Kolleg for Biology and Chemistry "Molecular Physiology", Heinrich-Heine-University of Düsseldorf.

[1] G. Wulff, A. Sarhan, K. Zabrocki, *Tetrahedron Lett.* **1973**, *44*, 4329–4332.
[2] G. Wulff, A. Sarhan, German patent, Offenlegungsschrift DE A 2242796, **1974**, [*Chem. Abstr.* **1975**, *83*, P 60300w]; US Patent, continuation in part US-A 4127730, **1978**.
[3] G. Wulff, *Angew. Chem.* **1995**, *107*, 1958—1979; *Angew. Chem. Int. Ed. Engl.* **1995**, *34*, 1812–1832.
[4] "Molecular and Ionic Recognition with Imprinted Polymers" (Eds.; R. A. Bartsch, M. Maeda), *ACS Symp. Ser. Vol 703*, Washington, **1998**.
[5] *Molecularly Imprinted Polymers—Man-Made Mimics of Antibodies and their Application in Analytical Chemistry* (Ed.: B. Sellergren), Elsevier, Amsterdam, **2001**.
[6] R. A. Lerner, S. J. Benkovic, P. G. Schultz, *Science* **1991**, *252*, 659–667.
[7] P. G. Schultz, *Angew. Chem.* **1989**, *101*, 1336–1348; *Angew. Chem. Int. Ed. Engl.* **1989**, *28*, 1283–1295.
[8] X.-C. Liu, K. Mosbach, *Macromol. Rapid Commun.* **1997**, *18*, 609–615.
[9] G. Wulff, T. Groß, R. Schönfeld, *Angew. Chem.* **1997**, *109*, 2049–2052; *Angew. Chem. Int. Ed. Engl.* **1997**, *36*, 1961–1964.
[10] B. Sellergren, K. J. Shea, *Tetrahedron: Asymmetry* **1994**, *5*, 1403–1406.
[11] B. Sellergren, R. N. Karmalkar, K. J. Shea, *J. Org. Chem.* **2000**, *65*, 4009–4027.
[12] K. Ohkubo, Y. Funakoshi, Y. Urata, S. Hirota, S. Usui, T. Sagawa, *J. Chem. Soc. Chem. Commun.* **1995**, 2143–2144.
[13] G. Wulff, *Chem. Rev.* **2002**, *102*, 1–28.
[14] G. Wulff, R. Schönfeld, *Adv. Mater.* **1998**, *10*, 957–959.
[15] G. Wulff, K. Knorr, *Bioseparation* **2002**, *10*, 257–276.
[16] J. D. Stewart, L. J. Liotta, S. J. Benkovic, *Acc. Chem. Res.* **1993**, *26*, 396–404.
[17] A. G. Strikovsky, D. Kasper, M. Grün, B. S. Green, J. Hradil, G. Wulff, *J. Am. Chem. Soc.* **2000**, *122*, 6295–6296.
[18] a) W. Chen, D. K. Han, K. D. Ahn, J. M. Kim, *Macromol. Res.* **2002**, *10*, 122–126b) J. M. Kim, K. D. Ahn, G. Wulff, *Macromol. Chem. Phys.* **2001**, 1105–1108.
[19] a) B. Castro, G. Evin, C. Selve, R. Seyer, *Synthesis* **1977**, 413; b) B. Castro, J. R. Dormoy, G. Evin, C. Selve, *Tetrahedron Lett.* **1975**, 1219–1222.
[20] J. Coste, E. Frérot, P. Jouin, *J. Org. Chem.* **1994**, *59*, 2437–2446.
[21] P. Kafarski, B. Lejczak, J. Szewczyk, *Can. J. Chem.* **1983**, *61*, 2425–2430.
[22] A. B. Smith, K. M. Yager, C. M. Taylor, *J. Am. Chem. Soc.* **1995**, *117*, 10879–10888.
[23] V. A. Solodenko, T. N. Kasheva, V. P. Kukhar, E. V. Kozlova, D. A. Mironenko, V. K. Svedas, *Tetrahedron* **1991**, *47*, 3989–3998.
[24] J. Szewczyk, B. Lejczak, P. Kafarski, *Synthesis* **1982**, *5*, 409–412.
[25] H. Bisswanger, *Enzyme Kinetics—Principles and Methods*, Wiley-VCH, Weinheim, **2002**.
[26] a) A. Cornish-Bowden, *Fundamentals of Enzyme Kinetics*, Portland Press, London, **1996**; b) P. J. F. Hernderson, in *Enzyme Assays* (Eds.: R. Eisenthal, M. J. Danson), IRL, Oxford, **1992**.
[27] G. Wulff, A. Biffis, in *Molecularly Imprinted Polymers—Man-Made Mimics of Antibodies and their Application in Analytical Chemistry* (Ed.: B. Sellergren), Elsevier, Amsterdam, **2001**, pp. 71–111.
[28] a) G. Wulff, in *Templated Organic Synthesis* (Eds. F. Diederich, P. J. Stang), Wiley-VCH, Weinheim, **1999**, pp. 39–73; b) G. Wulff, R. Schönfeld, M. Grün, R. Baumstark, G. Wildburg, L. Häussling, German Patent, Offenlegungsschrift DE A 19720345 A1, **1998**[*Chem. Abstr.* **1998**, *128* P 49155].

Received: January 28, 2003 [F4783]

